Organic & Biomolecular Chemistry

c9ob01545k

We have presented the Graphical Abstract text and image for your article below. This brief summary of your work will appear in the contents pages of the issue in which your article appears.

1

Norbornadiene–dihydroazulene conjugates

Martin Drøhse Kilde, Mads Mansø, Nicolai Ree, Anne Ugleholdt Petersen, Kasper Moth-Poulsen, Kurt V. Mikkelsen* and Mogens Brøndsted Nielsen*

Conjugates of norbornadiene (NBD) and dihydroazulene (DHA) photoswitches were synthesised and subjected to isomerisation studies.

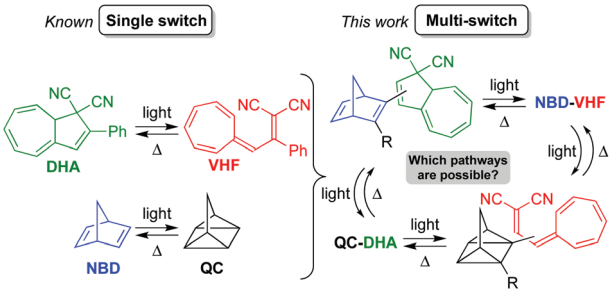

Please check this proof carefully. Our staff will not read it in detail after you have returned it.

Please send your corrections either as a copy of the proof PDF with electronic notes attached or as a list of corrections. **Do not edit the text within the PDF or send a revised manuscript** as we will not be able to apply your corrections. Corrections at this stage should be minor and not involve extensive changes.

Proof corrections must be returned as a single set of corrections, approved by all co-authors. No further corrections can be made after you have submitted your proof corrections as we will publish your article online as soon as possible after they are received.

Please ensure that:

- The spelling and format of all author names and affiliations are checked carefully. You can check how we have identified the authors' first and last names in the researcher information table on the next page. **Names will be indexed and cited as shown on the proof, so these must be correct.**
- Any funding bodies have been acknowledged appropriately and included both in the paper and in the funder information table on the next page.
- All of the editor's queries are answered.
- Any necessary attachments, such as updated images or ESI files, are provided.

Translation errors can occur during conversion to typesetting systems so you need to read the whole proof. In particular please check tables, equations, numerical data, figures and graphics, and references carefully.

Please return your **final** corrections, where possible within **48 hours** of receipt, by e-mail to: obc@rsc.org. If you require more time, please notify us by email.

Funding information

Providing accurate funding information will enable us to help you comply with your funders' reporting mandates. Clear acknowledgement of funder support is an important consideration in funding evaluation and can increase your chances of securing funding in the future.

We work closely with Crossref to make your research discoverable through the Funding Data search tool (http://search.crossref.org/funding). Funding Data provides a reliable way to track the impact of the work that funders support. Accurate funder information will also help us (i) identify articles that are mandated to be deposited in **PubMed Central (PMC)** and deposit these on your behalf, and (ii) identify articles funded as part of the **CHORUS** initiative and display the Accepted Manuscript on our web site after an embargo period of 12 months.

Further information can be found on our webpage (http://rsc.li/funding-info).

What we do with funding information

We have combined the information you gave us on submission with the information in your acknowledgements. This will help ensure the funding information is as complete as possible and matches funders listed in the Crossref Funder Registry.

If a funding organisation you included in your acknowledgements or on submission of your article is not currently listed in the registry it will not appear in the table on this page. We can only deposit data if funders are already listed in the Crossref Funder Registry, but we will pass all funding information on to Crossref so that additional funders can be included in future.

Please check your funding information

The table below contains the information we will share with Crossref so that your article can be found *via* the Funding Data search tool. **Please check that the funder names and grant numbers in the table are correct and indicate if any changes are necessary to the Acknowledgements text.**

Funder name	Funder's main country of origin	Funder ID (for RSC use only)	Award/grant number
Q1 Københavns Universitet	Denmark	501100001734	Unassigned

Researcher information

Please check that the researcher information in the table below is correct, including the spelling and formatting of all author names, and that the authors' first, middle and last names have been correctly identified. **Names will be indexed and cited as shown on the proof, so these must be correct.**

If any authors have ORCID or ResearcherID details that are not listed below, please provide these with your proof corrections. Please ensure that the ORCID and ResearcherID details listed below have been assigned to the correct author. Authors should have their own unique ORCID iD and should not use another researcher's, as errors will delay publication.

Please also update your account on our online manuscript submission system to add your ORCID details, which will then be automatically included in all future submissions. See here for step-by-step instructions and more information on author identifiers.

First (given) and middle name(s)	Last (family) name(s)	ResearcherID	ORCID iD
Martin Drøhse	Kilde		
Mads	Mansø		
Nicolai	Ree	C-6554-2018	0000-0001-9900-5730
Anne Ugleholdt	Petersen		
Kasper	Moth-Poulsen	A-6178-2009	0000-0003-4018-4927
Kurt V.	Mikkelsen	E-6765-2015	0000-0003-4090-7697
Mogens Brøndsted	Nielsen	G-1542-2014	0000-0001-8377-0788

Queries for the attention of the authors

Journal: **Organic & Biomolecular Chemistry** Paper: **c9ob01545k**

Title: **Norbornadiene–dihydroazulene conjugates**

For your information: You can cite this article before you receive notification of the page numbers by using the following format: (authors), Org. Biomol. Chem., (year), DOI: 10.1039/c9ob01545k.

Editor's queries are marked like this Q1, Q2, and for your convenience line numbers are indicated like this 5, 10, 15, ...

Please ensure that all queries are answered when returning your proof corrections so that publication of your article is not delayed.

Query Reference	Query	Remarks
Q1	Funder details have been incorporated in the funder table using information provided in the article text. Please check that the funder information in the table is correct.	
Q2	Please confirm that the spelling and format of all author names is correct. Names will be indexed and cited as shown on the proof, so these must be correct. No late corrections can be made.	
Q3	The sentence beginning "With the increasing demand..." has been altered for clarity, please check that the meaning is correct.	
Q4	The sentence beginning "However, the formation of..." has been altered for clarity, please check that the meaning is correct.	
Q5	In the sentence beginning "Moreover, excitation of NBD...", a word or phrase appears to be missing after "energy transfer". Please check this carefully and indicate any changes required here.	
Q6	Please note that a conflict of interest statement is required for all manuscripts. Please read our policy on Conflicts of interest (http://rsc.li/conflicts) and provide a statement with your proof corrections. If no conflicts exist, please state that "There are no conflicts to declare".	
Q7	Please check that ref. 6 has been displayed correctly.	

Organic & Biomolecular Chemistry

PAPER

Norbornadiene–dihydroazulene conjugates†

Cite this: DOI: 10.1039/c9ob01545k

Martin Drøhse Kilde,‡[a] Mads Mansø,‡[a,b] Nicolai Ree,[a] Anne Ugleholdt Petersen,[a] Kasper Moth-Poulsen,[b] Kurt V. Mikkelsen*[a] and Mogens Brøndsted Nielsen*[a]

Received 11th July 2019,
Accepted 25th July 2019

DOI: 10.1039/c9ob01545k

rsc.li/obc

The introduction of various photochromic units into the same molecule is an attractive approach for the development of novel molecular solar thermal (MOST) energy storage systems. Here, we present the synthesis and characterisation of a series of covalently linked norbornadiene/dihydroazulene (NBD/DHA) conjugates, using the Sonogashira coupling as the key synthetic step. Generation of the fully photoisomerized quadricyclane/vinylheptafulvene (QC/VHF) isomer was found to depend strongly on how the two units are connected – by linear conjugation (a *para*-phenylene bridge) or cross-conjugation (a *meta*-phenylene bridge) or by linking to the five- or seven-membered ring of DHA – as well as on the electronic character of another substituent group on the NBD unit. When the QC–VHF system could be reached, the QC-to-NBD back-reaction occurred faster than the VHF-to-DHA back-reaction, while the latter could be promoted simply by the addition of Cu(I) ions. The absence or presence of Cu(I) can thus be used to control whether heat releases should occur on different or identical time scales. The experimental findings were rationalized in a computational study by comparing natural transition orbitals (NTOs). Moreover, the calculations revealed an energy storage capacity of 106–110 kJ mol^{-1} of the QC–VHF isomers, which is higher than the sum of the capacities of the individual, separate units. The major contribution to the energy storage relates to the energetic QC form, while the major contribution to the absorption of visible light originates from the DHA photochrome; some of the NBD–DHA conjugates had absorption onsets at 450 nm or beyond.

Introduction

With the increasing demand for energy in the world, environmentally friendly energy resources are a necessity. The Sun provides limitless energy although the major challenge is to store the energy and release it when needed. Photochromic molecules, which upon light irradiation convert from low-energy isomers to high-energy, metastable isomers, have attracted increasing interest in recent years as an opportunity for storing solar energy. Such molecular systems are often termed molecular solar thermal (MOST) systems or solar thermal fuels (STF).[1] This principle is to absorb the Sun's radiant energy and store it as chemical energy in the chemical bonds of the metastable isomers that thermally convert back over time. Two important criteria for a functional system are to have absorbance matching the solar spectrum, ideally around 590 nm, and low molecular weight resulting in high energy density.[2]

Among the most studied photo-/thermoswitches for MOST applications are *trans*/*cis*-azobenzene (AZB),[1d,3] norbornadiene/quadricyclane (NBD/QC)[2a,4] and dihydroazulene/vinylheptafulvene (DHA/VHF)[5] couples (Scheme 1), but other systems have also been explored.[6] Some of us have recently shown that covalently linking together several NBDs results in improved energy densities, redshifted absorptions, and the possibility

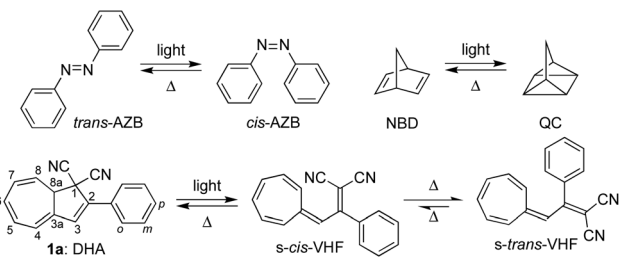

Scheme 1 Examples of MOST systems. Top left: *trans*-Azobenzene/*cis*-azobenzene (*trans*-AZB/*cis*-AZB). Top right: Norbornadiene/quadricyclane (NBD/QC). Bottom: Dihydroazulene/vinylheptafulvene (DHA/VHF).

[a]*Department of Chemistry, University of Copenhagen, Universitetsparken 5, DK-2100 Copenhagen Ø, Denmark. E-mail: kmi@chem.ku.dk, mbn@chem.ku.dk*
[b]*Department of Chemistry and Chemical Engineering, Chalmers University of Technology, Kemivägen 10, 412 96 Gothenburg, Sweden*

† Electronic supplementary information (ESI) available: NMR and UV-Vis absorption spectra (including switching studies), computational details. See DOI: 10.1039/c9ob01545k

‡ These authors contributed equally to this work.

for stepwise switching.[4b] Stepwise forward and/or backward switchings were also observed in acyclic and macrocyclic DHA dimers.[7] In the macrocyclic structures, stepwise energy releases corresponded to an initially fast discharge, hypothetically addressing thermal applications on different time scales with an initial immediate energy release (hours), and a subsequent slow process (days or weeks). To explore the concept of multimode switching further and to harvest a broader region of UV-visible light, we decided to create a new class of hybrid MOST chromophore systems by the linkage of NBD and DHA photoswitches. This is a rare combination of traditional and inverse photochromes both capable of storing significant amounts of heat. Herein, we present the synthesis, physicochemical characterisation and computational modelling of a series of six such conjugates expanding our knowledge of hybrid multichromophores for solar energy storage applications.

Results and discussion

Synthesis

An array of NBD/QC–DHA/VHF conjugates was conveniently prepared from previously reported DHA derivatives **1a**,[8] **1b**,[9] **1c**,[10] **1d**,[11] **1e**,[12] and **1f**[10] and NBD derivatives **2a**[13] and **2b**[14] (Schemes 2 and 3). First, NBD–DHAs $\mathbf{3a_{NBD-DHA}}$–$\mathbf{5a_{NBD-DHA}}$ with a phenyl substituent on the NBD was synthesized according to Scheme 1. DHA **1a** was subjected to a well-established bromination–elimination protocol,[15] providing a bromofunctionalized intermediate, which was used directly in a Sonogashira coupling with **2a** giving $\mathbf{3a_{NBD-DHA}}$ in 9% yield over 3 steps. DHAs **1b** and **1c** were converted under similar coupling conditions into conjugates $\mathbf{4a_{NBD-DHA}}$ and $\mathbf{5a_{NBD-DHA}}$ in yields of 61% and 51%, respectively. The second series of NBD–DHAs $\mathbf{3b_{NBD-DHA}}$–$\mathbf{5b_{NBD-DHA}}$ with a cyano group on the NBD was synthesized according to Scheme 3. First, the acetylenic DHAs **1d** and **1e** were desilylated using tetrabutylammonium fluoride (TBAF) in AcOH and THF, and the terminal alkyne intermediate was then coupled with **2b**, which resulted in products $\mathbf{3b_{NBD-DHA}}$ and $\mathbf{4b_{NBD-DHA}}$ in yields of 10% and 31%, respectively. DHA **1f** was subjected to identical coupling conditions providing $\mathbf{5b_{NBD-DHA}}$ in a yield of 79%. In these coupling reactions, the homo-coupled dimers **6–8** were isolated as by-products.

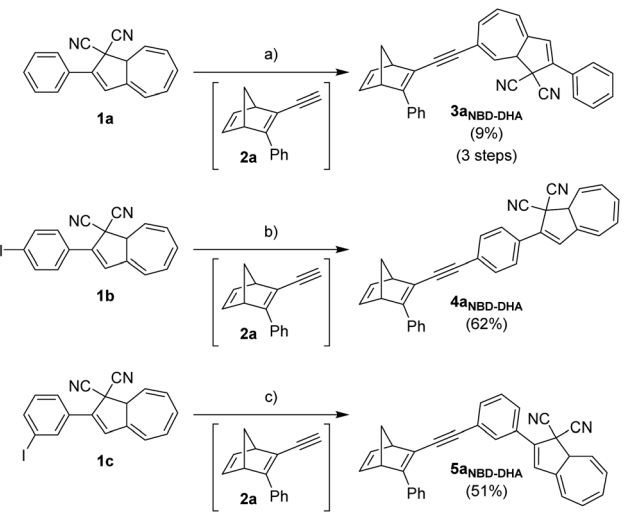

Scheme 2 Synthesis of NBD–DHA conjugates $\mathbf{3a_{NBD-DHA}}$, $\mathbf{4a_{NBD-DHA}}$ and $\mathbf{5a_{NBD-DHA}}$. Reagents and conditions (a) (1) Br_2, CH_2Cl_2, −78 °C, (2) LiHMDS, THF, 0 °C, (3) **2a**, $Pd(PPh_3)_2Cl_2$ (10 mol%), CuI (10 mol%), $(iPr)_2NH$/THF. (b) **2a**, $Pd(PPh_3)_2Cl_2$ (10 mol%), CuI (11 mol%), $(iPr)_2NH$/THF. (c) **2a**, $Pd(PPh_3)_2Cl_2$ (45 mol%), CuI (49 mol%), $(iPr)_2NH$/THF. LiHMDS = lithium hexamethyldisilazide.

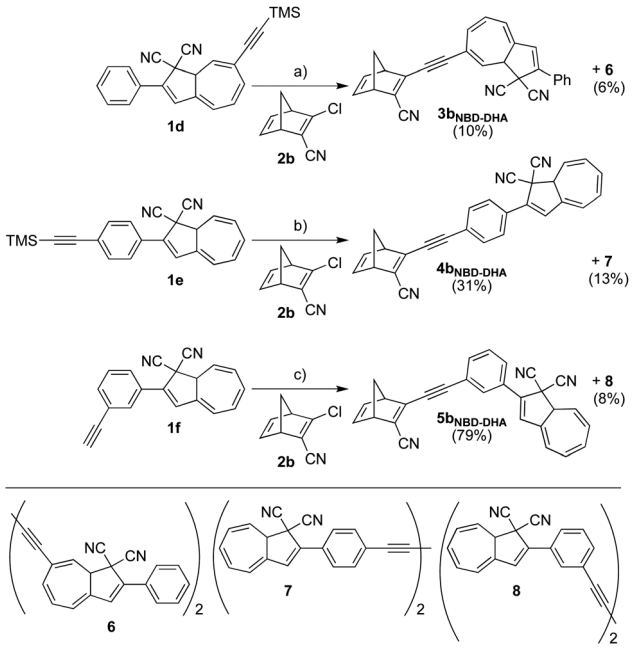

Scheme 3 Synthesis of NBD–DHA conjugates $\mathbf{3b_{NBD-DHA}}$, $\mathbf{4b_{NBD-DHA}}$ and $\mathbf{5b_{NBD-DHA}}$. Reagents and conditions (a) (1) TBAF, AcOH, THF, (2) **2b**, $Pd(PPh_3)_2Cl_2$ (10 mol%), CuI (13 mol%), $(iPr)_2NH$/THF. (b) (1) TBAF, AcOH, THF, (2) **2b**, $Pd(PPh_3)_2Cl_2$ (10 mol%), CuI (10 mol%), $(iPr)_2NH$/THF. (c) **2b**, $Pd(PPh_3)_2Cl_2$ (10 mol%), CuI (10 mol%), $(iPr)_2NH$/THF.

UV-Vis absorption spectroscopy and switching studies

Fig. 1 summarizes the absorption properties of previously studied compounds. The unsubstituted NBD has an absorption onset at 267 nm and a maximum far in the UV region, which can be redshifted upon addition of functional groups across one of the double bonds as seen in compounds **9** and **10** (Fig. 1).[14] DHA **1a** has an absorption onset at 452 nm (the onset is defined as ε = 100 M^{-1} cm^{-1}) and a maximum at 360 nm (toluene),[8] hence redshifted relative to the unsubstituted NDB and derivatives **9** and **10**. Its corresponding, non-photoactive VHF isomer has a characteristic absorption maximum at 464 nm. Substitution of DHA at the phenyl group or at position C7 has in several examples been shown to have little effect in regard to the longest-wavelength DHA absorption.[10,11,15] However, the DHA dimer **11** with a *p*-pheny-

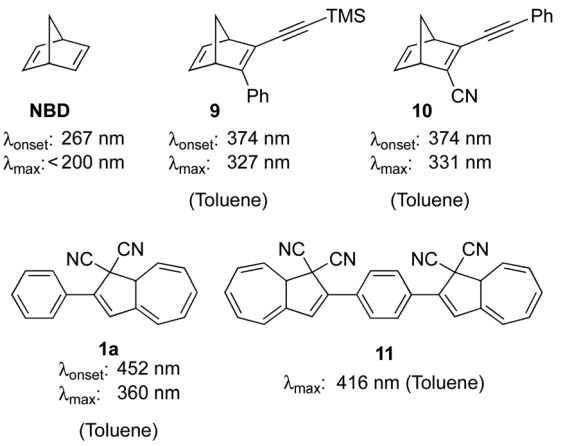

Fig. 1 Selection of known NBDs and DHA **1a** with their absorption onsets and maxima.

lene bridge connecting the C2 positions of each DHA exhibited a significantly redshifted absorption maximum at 416 nm and reduced photoswitching capacity.[7a]

With the two novel series of **3a–5a**/**3b–5b** in hand, the optical and switching properties were studied in detail by UV-Vis absorption spectroscopy in toluene. Absorption maxima (λ_{max}), molar absorptivities (ε), VHF-to-DHA half-lives and QC-to-NBD half-lives ($t_{\frac{1}{2}}$) are listed in Table 1. Compounds **4a** and **4b** with a linearly conjugated bridge between the NBD and DHA units stand out as those with the longest-wavelength absorptions among the NBD–DHA isomers, with maxima at 406 and 392 nm, respectively, close to the maximum exhibited by DHA dimer **11** (416 nm) and signaling a strong interaction between the two units, in line with a natural transition orbital analysis (*vide infra*). The other NBD–DHA chromophores had the longest-wavelength absorption maximum in the region 345–361 nm, close to that of DHA **1a** (360 nm).

All photoisomerizations were conducted at 25 °C, while the thermal back-reactions were studied at 50 °C. A schematic presentation of the possible switching events is shown in Scheme 4, including a brief overview of the outcome of the studies described below. Absorption spectra of NBD–DHAs $\mathbf{3a/b_{NBD–DHA}}$–$\mathbf{5a/b_{NBD–DHA}}$, NBD–VHFs $\mathbf{3a/b_{NBD–VHF}}$–$\mathbf{5a/b_{NBD–VHF}}$ and QC–VHFs $\mathbf{4b_{QC–VHF}}$, $\mathbf{5a_{QC–VHF}}$ and $\mathbf{5b_{QC–VHF}}$ are shown in Fig. 2, and data are listed in Table 1. UV-Vis absorption spectra corresponding to all the photo-/thermoswitching experiments can be found in the ESI.†

Initially, all the NBD–DHA systems were subjected to irradiation around the longest-wavelength absorption onset, corresponding to the onset of the respective DHA subunits ($\mathbf{3a/b_{NBD–DHA}}$ and $\mathbf{5a/b_{NBD–DHA}}$: 400 nm, $\mathbf{4a/b_{NBD–DHA}}$: 450 nm), ensuring photochemical conversion to the NBD–VHF states. All conjugates $\mathbf{3a/b_{NBD–DHA}}$–$\mathbf{5a/b_{NBD–DHA}}$ were found to easily undergo photochemically induced ring-opening of the DHA scaffold to generate the NBD–VHF form, as seen by the distinct VHF absorption band arising around 470 nm (close to that of $\mathbf{1a_{VHF}}$ at 464 nm (ref. 8)) accompanied by a decrease in the characteristic DHA absorption band around 360 nm. In addition, ^{1}H NMR spectroscopic studies performed in toluene-d_8 (at concentrations of 10^{-2}–10^{-3} M) of all six DHA–NBD compounds verified that irradiation at the onset of the respective DHA subunits solely led to the conversion of the DHA subunit to the VHF and no conversion of the NBD subunit to QC (see ESI Fig. S25–S39†). The VHFs are not photo-active, but VHF-to-DHA ring-closures back to the initial NBD–DHA states were successfully achieved thermally. Both the ring-opening and ring-closure events appeared with isosbestic points in the absorption spectra, indicating that only one reaction occurs each way (however, small degrees of decomposition of the systems cannot be excluded). By following the decay of VHF absorbance at 50 °C (first-order kinetics), the rate of back-reaction was obtained by curve fitting the data with a single-exponential fit. For the NBD–VHFs $\mathbf{4b_{NBD–VHF}}$ and $\mathbf{5b_{NBD–VHF}}$, the half-lives were similar (see Table 1), in the range of 50–70 min. For NBD–VHFs $\mathbf{3b_{NBD–VHF}}$ and $\mathbf{3b_{NBD–VHF}}$, the half-lives were longer, reaching almost 600 min for $\mathbf{3b_{NBD–VHF}}$. Thus, as seen before[11] an electron-withdrawing alkyne-linker placed on the seven-membered ring has a significant impact on the rate of

Table 1 UV-Vis absorption data (longest-wavelength absorption maxima) at 25 °C and VHF/QC half-lives at 50 °C in toluene. All QC half-lives originating from double exponential fits are obtained by locking the rate constant of the VHF conversion (k_1) obtained from an exponential fit of the decay of VHF absorption. Double exponential fits without locking the k_1 value are shown in the ESI.† sh = shoulder

	NBD–DHA	NBD–VHF		QC–VHF		
System	λ_{max} [nm] (ε [10^3 M^{-1} cm^{-1}])	λ_{max} [nm] (ε [10^3 M^{-1} cm^{-1}])	VHF-to-DHA $t_{\frac{1}{2}}$ [min] (50 °C)	λ_{max} [nm] (ε 10^3 [M^{-1} cm^{-1}])	VHF-to-DHA $t_{\frac{1}{2}}$ [min] (50 °C)	QC-to-NBD $t_{\frac{1}{2}}$ [min] (50 °C)
3a	358 (16.3)	509 (22.4)	146	—	—	—
3b	sh 365 (15.9) 335 (21.7)	478 (33.5)	587	—	—	—
4a	406 (27.5)	459 (21.5)	59	—	—	—
4b	392 (34.1)	473 (24.2)	52	349 (13.4)	45[a], 53[b]	45[a], 12[c]
5a	361 (23.1)	467 (21.7)	70	467 (21.9)	70[b,d]	11[c,d]
5b	345 (23.7)	469 (27.5)	53	469 (27.4)	45[a], 57[b]	45[a], 32[c]

[a] Data obtained from a single exponential fit of the growth of absorption of the NBD–DHA λ_{max}. [b] Data obtained from a single exponential fit of the decay of VHF absorption. [c] Data obtained from the sum of two exponential functions of the growth of the absorption of the NBD–DHA λ_{max}, locking the k_1 value (see eqn (1)) to that obtained from the decay of VHF absorption (of QC–VHF). [d] Data from the growth of absorbance at 355 nm could not be fitted with a single exponential fit (see ESI Fig. S47†).

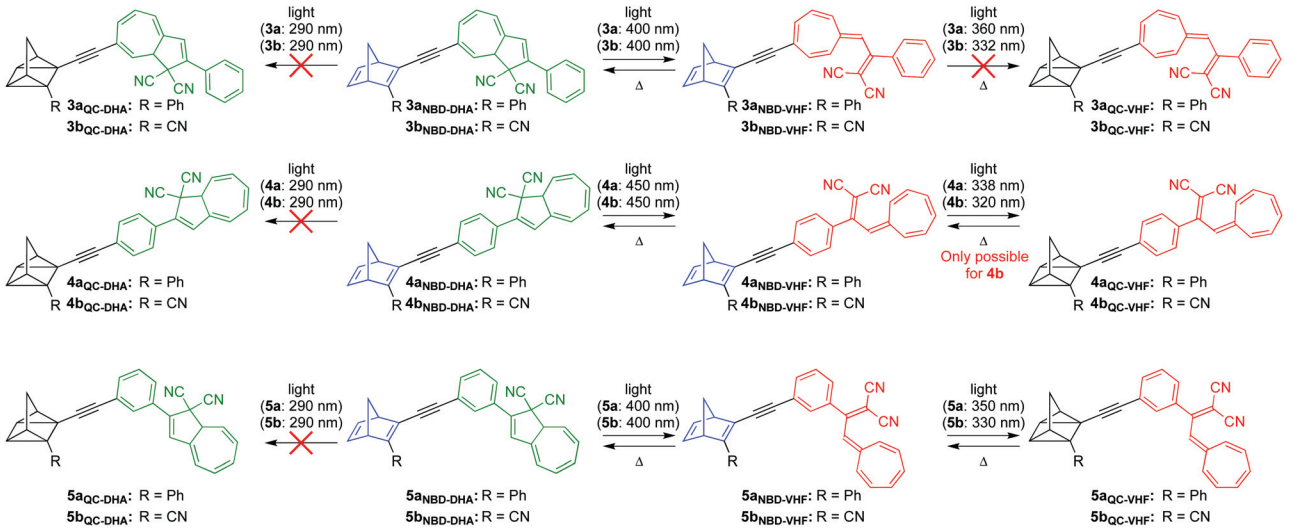

Scheme 4 Overview of the multimode switching events of compounds **3–5** in toluene.

back-reaction, and the "cyanoethylene" moiety present in **3b** enhances the electron-withdrawing effect further. As previously reported[11] for 7-substituted DHAs, *E*/*Z* isomerization around the exocyclic double bond of the VHF results in the accumulation of the 6-substituted isomer upon several photo/thermal cycles (see ESI Fig. S42†). For all the NBD–DHAs **3a/b$_{NBD–DHA}$**–**5a/b$_{NBD–DHA}$** light irradiation at 290 nm in toluene (an absorption cut-off ~290 nm) resulted in selective isomerization of the DHA unit to form the NBD–VHF states. Changing the solvent to cyclohexane (an absorption cut-off ~190 nm) allowed for shorter wavelength (220–240 nm) light to be used. However, the formation of NBD–VHF isomers was obtained in all cases **3–5**. In an attempt to reach the QC–VHF state, all of the formed NBD–VHFs were irradiated in toluene at the local maxima (**3a$_{NBD–VHF}$**: 360 nm, **3b$_{NBD–VHF}$**: 332 nm, **4a$_{NBD–VHF}$**: 338 nm, **4b$_{NBD–VHF}$**: 320 nm, **5a$_{NBD–VHF}$**: 350 nm, **5b$_{NBD–VHF}$**: 330 nm). In this case, a gradual decrease in the characteristic absorptions at around 320 nm (**4b$_{NBD–VHF}$**), 350 nm (**5a$_{NBD–VHF}$**), and 330 nm (**5b$_{NBD–VHF}$**) was observed for compounds **4b$_{NBD–VHF}$**, **5a$_{NBD–VHF}$**, and **5b$_{NBD–VHF}$**, corresponding to light-induced conversion from the NBD–VHF state to the QC–VHF state. Irradiation of the respective compounds **4b$_{NBD–VHF}$** (320 nm), **5a$_{NBD–VHF}$** (350 nm) and **5b$_{NBD–VHF}$** (330 nm) was performed until no changes in the absorption spectrum were observed (corresponding to either full conversion to the QC–VHF state or a photostationary state between the QC–VHF and NBD–VHF states). For NBD–VHFs **3a$_{NBD–VHF}$**, **3b$_{NBD–VHF}$**, and **4a$_{NBD–VHF}$**, no sign of isomerization to the QC–VHF state was observed. Irradiation at various wavelengths between 290 nm and 400 nm resulted only in photodegradation of the three systems. For comparison, we also subjected a 1 : 1 mixture of DHA **1a** and NBD **9** to irradiation at 404 nm until the complete conversion of the **1a$_{DHA}$** into **1a$_{VHF}$**. Subsequently, **9$_{NBD}$** was successfully photoisomerized into **9$_{QC}$** by irradiation at 320 nm. In consequence, the lack of NBD-to-QC photoisomerization of **3a$_{NBD–VHF}$**, **3b$_{NBD–VHF}$**, and **4a$_{NBD–VHF}$** originates from an intramolecular effect rather than from an intermolecular effect. Subsequently, we followed the switching capabilities (the NBD–VHF state to the QC–VHF state) by NMR spectroscopy in toluene-d_8. Firstly, a 1 : 1 mixture of DHA **1a** and NBD **9** (10^{-2} M) was easily converted from **1a$_{DHA}$** into **1a$_{VHF}$** (with no change of NBD **9**) using 415 nm light, and thereafter **9$_{NBD}$** was successfully converted into **9$_{QC}$** using 340 nm light. Secondly, after the formation of the NBD–VHF state of all compounds **3–5**, we subjected these NMR samples to light irradiation at 340 nm. For **5b$_{NBD–VHF}$**, we estimate that roughly 70% was converted into **5b$_{QC–VHF}$**. For the other NBD–VHF compounds, no sign of isomerization could be observed in the ^{1}H NMR spectra; only decomposition of the NMR samples was observed upon prolonged irradiation (see ESI Fig. S25–S39†). We assign the lack of isomerization of **4b$_{NBD–VHF}$** and **5a$_{NBD–VHF}$** on the NMR scale to a combination of low NBD-to-QC photoisomerization quantum yields as well as to the increased concentrations required for the NMR studies compared to the UV-Vis studies (a difference of 2–3 orders of magnitude), where switchings of **4b$_{NBD–VHF}$** and **5a$_{NBD–VHF}$** were indeed observed.

Gratifyingly, as mentioned above, irradiation of the *para*-linked **4b$_{NBD–VHF}$** and both of the *meta*-linked NBD–VHFs **5a$_{NBD–VHF}$** and **5b$_{NBD–VHF}$** at their local maxima resulted in full or part isomerization to their corresponding QC–VHFs when followed by UV-Vis absorption spectroscopy at concentrations of 10^{-5} M. This could be seen by a decrease in absorbance at the local maximum while the VHF absorbance remained unchanged. After cyclization to the QC–VHFs, the thermal back-reaction to the NBD–DHAs was followed. The half-life of VHF-to-DHA in the three QC–VHF systems (**4b$_{QC–VHF}$**, **5a$_{QC–VHF}$** and **5b$_{QC–VHF}$**) could be easily obtained by following the decay of VHF-absorbance, as there are no interfering absorbance bands in this region (around 470 nm). When following the

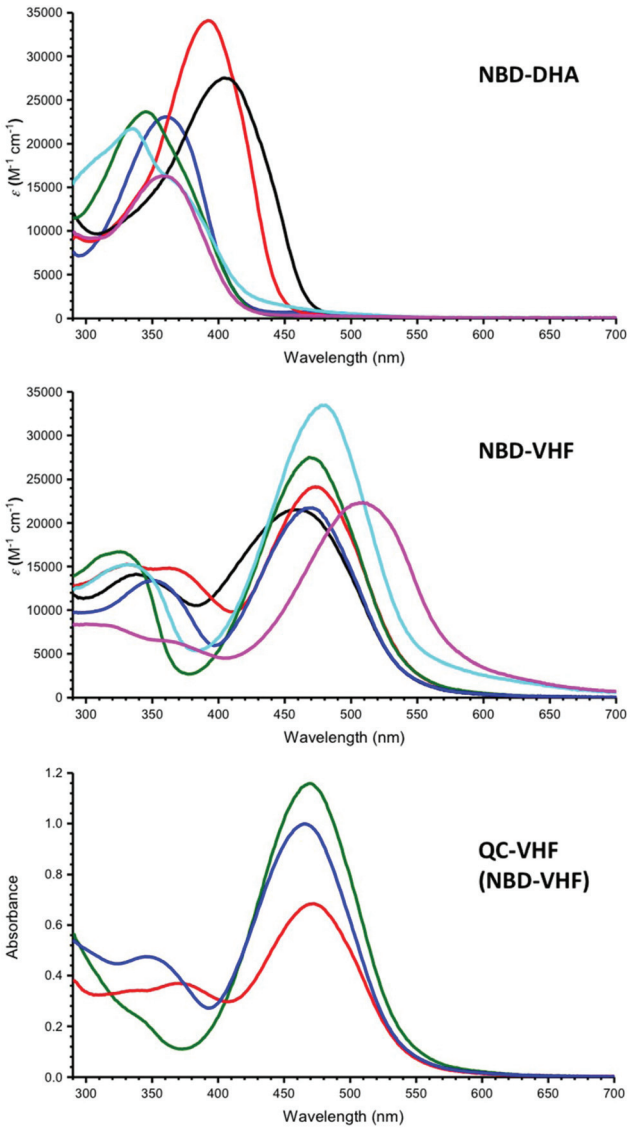

Fig. 2 UV/Vis absorption spectra recorded at 25 °C in toluene at concentrations of 10^{-5} M. Top: Spectra of NBD–DHA systems: $\mathbf{3a}_{\mathbf{NBD-DHA}}$ (magenta), $\mathbf{3b}_{\mathbf{NBD-DHA}}$ (cyan), $\mathbf{4a}_{\mathbf{NBD-DHA}}$ (black), $\mathbf{4b}_{\mathbf{NBD-DHA}}$ (red), $\mathbf{5a}_{\mathbf{NBD-DHA}}$ (blue), $\mathbf{5b}_{\mathbf{NBD-DHA}}$ (green). Middle: Spectra of NBD–VHF systems: $\mathbf{3a}_{\mathbf{NBD-VHF}}$ (magenta), $\mathbf{3b}_{\mathbf{NBD-VHF}}$ (cyan), $\mathbf{4a}_{\mathbf{NBD-VHF}}$ (black), $\mathbf{4b}_{\mathbf{NBD-VHF}}$ (red), $\mathbf{5a}_{\mathbf{NBD-VHF}}$ (blue), $\mathbf{5b}_{\mathbf{NBD-VHF}}$ (green). Bottom: Spectra of QC–VHF systems (or a photostationary state between the QC–VHF and NBD–VHF): $\mathbf{4b}_{\mathbf{QC-VHF}}$ (red), $\mathbf{5a}_{\mathbf{QC-VHF}}$ (blue), $\mathbf{5b}_{\mathbf{QC-VHF}}$ (green).

decay of VHF-absorbance in the QC–VHF states, similar half-lives were obtained to that for the NBD–VHFs. Thus, the rate of VHF back-reaction seems to be independent of the NBD/QC state.

The half-life of QC-to-NBD in the three QC–VHF systems ($\mathbf{4b}_{\mathbf{QC-VHF}}$, $\mathbf{5a}_{\mathbf{QC-VHF}}$ and $\mathbf{5b}_{\mathbf{QC-VHF}}$) is more challenging to obtain as the NBD and DHA absorption bands are overlapping. However, as we know the rate of DHA formation (from the VHF decay rate), it is possible to estimate the kinetics of the QC-to-NBD conversions. For all the QC–VHF systems, an approximate half-life for the conversion of the QC moiety was obtained by following the growth of the absorbance peak around 340 nm (**4b**: 368 nm, **5a**: 355 nm, **5b**: 326 nm). The growth of absorbance in time, $A(t)$, was fitted as the sum of two exponential functions (eqn (1); where c_1 and c_2 are constants; k_1 and k_2 are the rate constants for VHF-to-DHA and QC-to-NBD conversions, respectively, and A_∞ is the absorbance at an infinite time). In this fitting procedure, the k_1 rate constants were kept fixed as the numbers obtained from the decay of VHF absorbance (corresponding to VHF half-lives of *ca.* 53, 70, and 57 min for **4b**, **5b**, and **5a**, respectively). Thereby, QC-to-NBD conversions were found to occur with half-lives of *ca.* 11–12 min (**4b**, **5a**) and *ca.* 32 min (**5b**).

Fitting the growth of the absorbance peak at around 340 nm with only one exponential function gives overall half-lives for the conversion of QC–VHF into NBD–DHA of *ca.* 45 min for **4b** and **5b**.

$$A(t) = c_1 e^{-k_1 t} + c_2 e^{-k_2 t} + A_\infty \quad (1)$$

Copper promoted back-reaction

To reach the QC–DHAs selectively, it was attempted to accelerate the back-reaction of the VHF moiety of the QC–VHF state. Lewis acids have shown to have a pronounced effect on the reversible switching of DHA/VHF systems. Hence, a strong Lewis acid such as $AlCl_3$ promotes ring-opening[16] (DHA-to-VHF), while a Cu(I) salt ($Cu(MeCN)_4BF_4$) greatly induces ring-closure[17] (VHF-to-DHA; data for **1a** are included in Table 2). Similarly, cobalt-based catalyst systems for the effective triggering of the QC-to-NBD conversion have been reported in the literature.[18] Furthermore, it was of interest to test whether the NBD/QC scaffold would show stability towards the Cu(I) salt, as an analogous NBD has shown instability in the presence of similar Cu(I) salts.[18] Compound **5a** was chosen (devoid of a cyano group at NBD), as it is postulated that the catalytic effect of the Cu(I) salt is mediated by coordination to the vinylic cyano groups of VHF. For comparison with the earlier studies

Table 2 Kinetics data for VHF-to-DHA and QC-to-NBD conversions at 25 °C in CH_2Cl_2 with and without the addition of $Cu(MeCN)_4BF_4$

	NBD–VHF	Cu@NBD–VHF	QC–VHF		Cu@QC–VHF	
Compound	VHF-to-DHA $t_{\frac{1}{2}}$ [min]	VHF-to-DHA $t_{\frac{1}{2}}$ [min]	VHF-to-DHA $t_{\frac{1}{2}}$ [min]	QC-to-NBD $t_{\frac{1}{2}}$ [min]	VHF-to-DHA $t_{\frac{1}{2}}$ [min]	QC-to-NBD $t_{\frac{1}{2}}$ [min]
1a	545	18–22[a]	—	—	—	—
5a	428	26[a], 8[b]	428[c]	3[d]	9[e]	—[b,f]

[a] In the presence of 1 equiv. of $Cu(MeCN)_4BF_4$. [b] In the presence of 8 equiv. of $Cu(MeCN)_4BF_4$. [c] Obtained from exponential growth of $\mathbf{5a}_{\mathbf{NBD-DHA}}$ at 355 nm after the 16th minute of back-reaction (see ESI Fig. S51†). [d] Obtained from exponential growth of the absorption of the NBD–DHA λ_{max} for the first 16 minutes of back-reaction (see ESI Fig. S51†). [e] Data obtained from a single exponential fit of the decay of the Cu@VHF absorption. [f] Data from exponential fits of the growth of absorption of the NBD–DHA λ_{max} did not show any definitive results (see ESI Fig. S53†).

on **1a**,[17] CH_2Cl_2 at 25 °C was used as the solvent. Firstly, the switching properties of **5a** in this solvent were investigated (see Table 2). Irradiation of $\mathbf{5a_{NBD-DHA}}$ at 400 nm resulted in isomerization to $\mathbf{5a_{NBD-VHF}}$. The decay of VHF absorbance was then followed and fitted with a single exponential fit, which provided a VHF-to-DHA half-life of 428 min. Complete photoisomerization to $\mathbf{5a_{QC-VHF}}$ could be obtained by irradiation of $\mathbf{5a_{NBD-VHF}}$ at 347 nm. Interestingly, the QC scaffold had a significantly increased rate of back-reaction in CH_2Cl_2 at 25 °C, resulting in a half-life of only 3 min (compared to 11 min in toluene at 50 °C). The VHF moiety in $\mathbf{5a_{QC-VHF}}$ had a similar half-life to that in $\mathbf{5a_{NBD-VHF}}$.

Addition of 1 equiv. of $Cu(MeCN)_4BF_4$ to $\mathbf{5a_{NBD-VHF}}$ in CH_2Cl_2 at 25 °C resulted in an almost 20-fold increase in the rate of the VHF-to-DHA back-reaction (Table 2). Thus, a half-life of 26 min was obtained, similar to that reported for **1a**.[17] Addition of 8 equiv. of the Cu(I) salt resulted in an almost 60-fold decrease in the VHF half-life (Scheme 5). Due to the markedly increased rate of back-reaction of the VHF moiety upon addition of 8 equiv. of the Cu(I) salt, these conditions were applied in the case of $\mathbf{5a_{QC-VHF}}$ in an attempt to reach the $\mathbf{5a_{QC-DHA}}$ state. However, owing to the fast rate of back-reaction of the QC moiety, $\mathbf{5a_{QC-DHA}}$ could not be reached. The half-life of the VHF moiety was obtained from a single exponential fit from the decay of the VHF absorption band. Unfortunately, it was not possible to obtain any conclusive results about the half-life of the QC moiety with the addition of 8 equiv. of the Cu(I) salt. However, an overall half-life ($\mathbf{5a_{QC-VHF}}$-to-$\mathbf{5a_{NBD-DHA}}$) of 9 min was obtained from the growth of the absorption band at 355 nm fitted by a single exponential function. Nevertheless, we suspect that the half-life of the QC subunit in $\mathbf{5a_{QC-VHF}}$ is 3 minutes or less.

Computational study

To understand why some NBD–VHFs ($\mathbf{4b_{NBD-VHF}}$, $\mathbf{5a_{NBD-VHF}}$ and $\mathbf{5b_{NBD-VHF}}$) could be fully photoconverted, while other conjugates could not ($\mathbf{3a_{NBD-VHF}}$, $\mathbf{3b_{NBD-VHF}}$ and $\mathbf{4a_{NBD-VHF}}$), we performed a computational study using time-dependent density functional theory (TD-DFT) at the CAM-B3LYP/6-311+G(d) level of theory in a dielectric medium of toluene (details are provided in the Experimental section). Fig. 3 shows the calculated natural transition orbitals (NTOs) and simulated UV-Vis absorption spectra of the lowest-energy conformers of **4a**, **4b**, **5a**, and **5b**, while calculated absorption spectra for **3a** and **3b** are shown in the ESI;† Gibbs free energies of the lowest-energy conformers of all compounds are also listed in the ESI.† The NTOs are the highest occupied transition orbitals (HOTOs) and the lowest unoccupied transition orbitals (LUTOs) that correspond to the transitions (labeled I and II) shown in the UV-Vis absorption spectra. The NTOs of the *para*-substituted system $\mathbf{4a_{NBD-VHF}}$ (green box) show that transition II is not localized on the NBD unit, but it involves the VHF unit to a large extent. This perturbation of the photochromic unit may explain its reluctance to undergo NBD-to-QC conversion; the system should not be considered to be isolated NBD and VHF units, with local excitations, but rather as a new chromophore. The NTOs of $\mathbf{4a_{NBD-DHA}}$ (blue box, top) show some extension of the DHA chromophore part, but as we see from the experiments, this more limited extension does not destroy the DHA-to-VHF photoactivity. For $\mathbf{4b_{NBD-VHF}}$ (green box, middle), transition II also involves part of the VHF unit, but not to the same significant degree as that observed for $\mathbf{4a_{NBD-VHF}}$, and, indeed, this compound was able to undergo the NBD-to-QC conversion.

The NTOs of the *meta*-substituted systems (**5a** and **5b**) show that the HOTOs and LUTOs are more localized on the two different chromophores for all the various forms. Indeed, these compounds were able to undergo both DHA-to-VHF and NBD-to-QC conversions. Decoupling of individual photoswitches using the *meta*-connectivity principle has also been recently explored in experimental and computational studies on *meta*-substituted bis- and trisazobenzenes.[19] The two transitions I and II of $\mathbf{5a_{NBD-DHA}}$ and $\mathbf{5b_{NBD-DHA}}$ (blue boxes), corresponding to the NBD-to-QC and DHA-to-VHF photoisomerizations, are rather close in energies. This agrees with the experimental finding that the NBD-to-QC conversion could not be done without an accompanying DHA-to-VHF conversion. Moreover, excitation of NBD may lead to energy transfer to DHA, inducing its photoisomerization into VHF. However, experimentally, the DHA-to-VHF conversion was in fact achieved selectively, which is not so easy to rationalize. Overall, the NTOs give a good qualitative picture of the switching capabilities of the individual systems that are in good agreement with the experimental findings, but, of course, the reaction progress on the excited-state energy surfaces is more complicated than the simplified picture we have used here to rationalize our experimental findings.

In the context of MOST systems, the energy storage capacity is an important parameter, that is, the energy difference between the low- and high-energy isomers. For systems **3–5**, an initial DHA-to-VHF isomerization causes a rather small increase in Gibbs free energy of 8–10 kJ mol^{-1} in toluene (based on the most stable s-*trans*-VHF conformer), while the second isomerization (NBD-to-QC) causes an additional, much

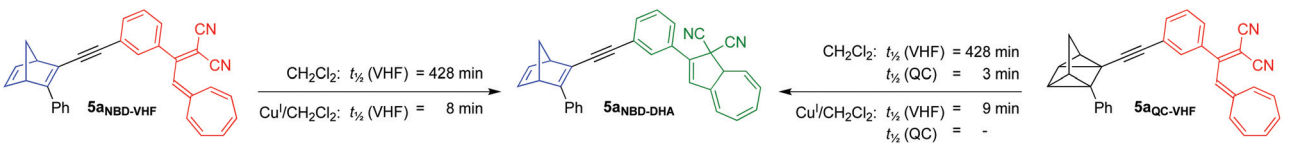

Scheme 5 Conversions (with half-lives listed) of compounds $\mathbf{5a_{NBD-VHF}}$ and $\mathbf{5a_{QC-VHF}}$ in CH_2Cl_2 in the absence or presence of $Cu(MeCN)_4BF_4$ (8 equiv.).

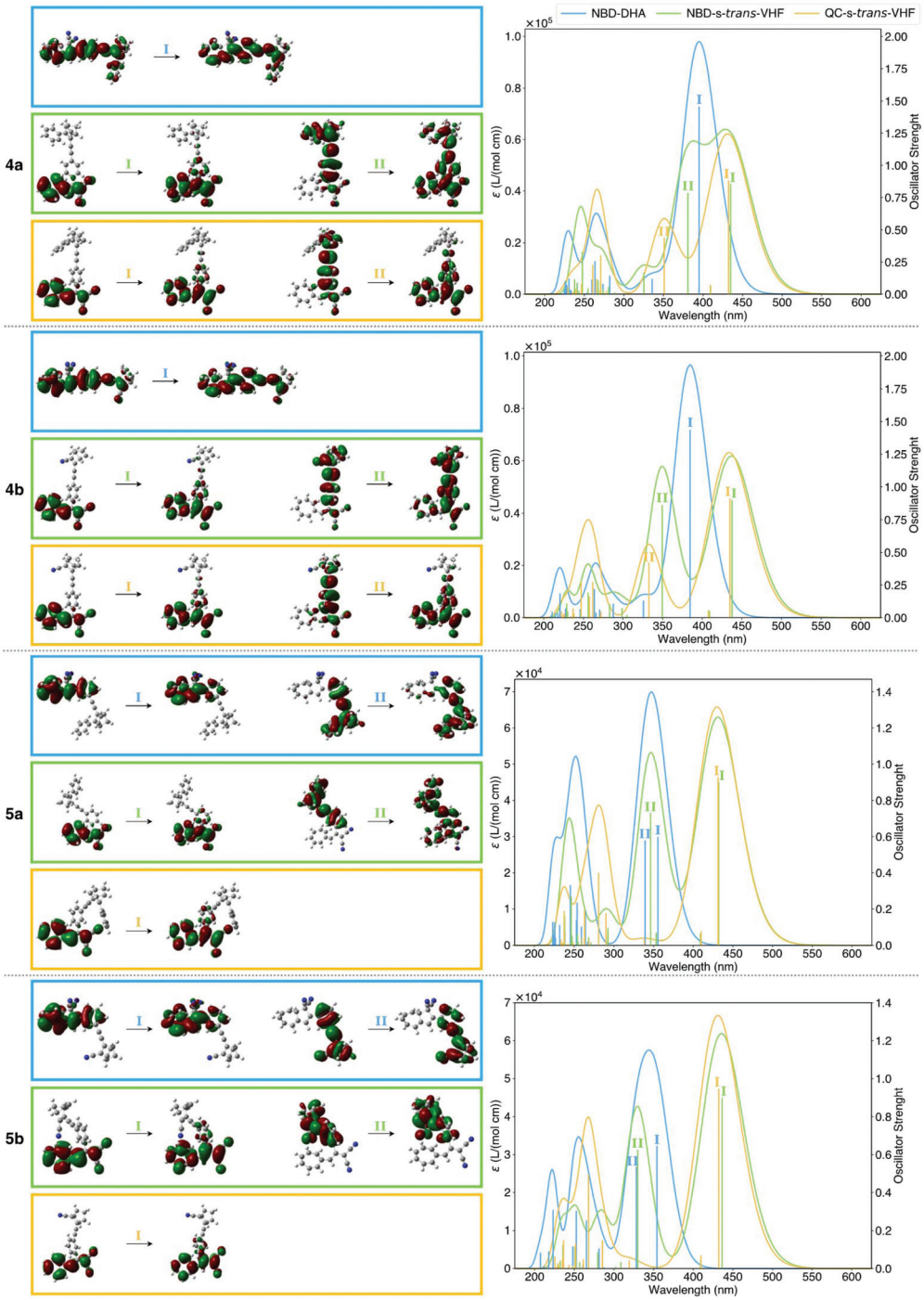

Fig. 3 Natural transition orbitals (NTOs) showing the highest occupied and lowest unoccupied transition orbitals for different transitions of the **4a**, **4b**, **5a**, and **5b** system. The transitions correspond to the excitations shown in the UV-Vis absorption spectra on the right-hand side, which are calculated using TD-DFT at the CAM-B3LYP/6-311+G(d) level of theory in a dielectric medium of toluene. The color-coding refers to the state of photoisomerization as indicated in the upper right-hand side corner.

larger increase of 96–101 kJ mol^{-1}. The storage capacity of the DHA-to-VHF isomerization is comparable to calculations at the same level of theory for the parent DHA/VHF system in a dielectric medium of cyclohexane (ε_{st} = 2.017 and ε_{op} = 2.035) with a storage capacity of 10 kJ mol^{-1}.[20] More surprisingly, the storage capacity of the NBD-to-QC isomerization is higher than that of the unsubstituted NBD/QC photothermal switch (see Scheme 1), which has a storage capacity of 88 kJ mol^{-1} at the same level of theory in a dielectric medium of toluene (see ESI Tables S1–S6†). These findings, therefore, prove the possibility

of linking the two photochromic units without losing their individual energy storage capacities (in kJ mol^{-1}), but in fact increase the overall capacity to more than the sum of the individual units, and moreover with the ability to enhance the solar spectrum match. When taking molecular weights into account, we get energy storage capacities for **4b**, **5a**, and **5b** (all of which could experimentally be converted into QC–VHF forms) of 0.27, 0.24, and 0.27 MJ kg^{-1} (in toluene); the number for **5a** is slightly lower on account of its higher molecular weight.

Experimental section

General procedures (experimental work)

All reagents and solvents were obtained from commercial suppliers and used as received unless otherwise stated. THF was collected from an IT (Innovative Technology) installation of model PS-MD-05. All air and moisture sensitive reactions were carried out under an inert atmosphere (argon gas). All handling of photochromic compounds was done in the dark. Purification by column chromatography was carried out on silica gel (flash column, SiO_2 40–63 μm). For purification of DHA compounds, all glassware was wrapped in tin foil to exclude compounds from light. Thin-layer chromatography (TLC) was carried out using commercially available aluminum sheets pre-coated with silica gel (silica 60) with a fluorescence indicator and visualized under UV light at 254 or 365 nm; color change from yellow to red upon irradiation with UV light (365 nm, not 254 nm) indicated the presence of DHA. All TLC analyses of DHA compounds were carried out in the dark by covering the TLC jar. All melting points are uncorrected. NMR spectroscopy was performed using a Bruker instrument equipped with a non-inverse cryoprobe at 500 MHz (^{1}H NMR) or 126 MHz (^{13}C NMR). Chemical shift values are quoted in ppm and coupling constants (J) in Hz. ^{1}H and ^{13}C NMR spectra are referenced against residual solvent peaks ($CDCl_3$: δ_H = 7.26 ppm and δ_C = 77.16 ppm). $CDCl_3$ was purchased unstabilized and passed through activated basic alumina prior to use. HRMS was recorded using an ESP-MALDI-FT-ICR spectrometer equipped with a 7 T magnet calibrated using NaTFA cluster ions. UV-Vis absorption spectra were recorded using a Varian Cary 50 Bio UV-vis spectrophotometer, performed in a 1 cm path-length cuvette, and the neat solvent was used as a baseline; sh = shoulder. Irradiation studies were performed using an ozone-free 450 W Xe lamp equipped with a monochromator when followed by UV-Vis absorption spectroscopy and using Thorlabs LED lamps M340L4, M365L2, M415L4 and M450LP1 (for wavelengths of 340, 365, 415 and 450 nm, respectively) when followed by NMR spectroscopy.

Compound $3a_{NBD–DHA}$ (isolated as a mixture of diastereoisomers). To a solution of **1a** (1.52 g, 5.93 mmol) in CH_2Cl_2 (150 mL) under an argon atmosphere at −78 °C was added a solution of Br_2 in CH_2Cl_2 (7.6 mL, 0.78 M, 5.9 mmol) dropwise. The reaction mixture was then stirred for 3 h, after which it was raised from the cooling bath and allowed to reach rt. Evaporation of the solvents gave the dibromide intermediate, which was then dried under high vacuum for 0.5 h. The dibromide was dissolved in dry THF (100 mL) under an argon atmosphere and cooled to 0 °C after which a solution of LiHMDS in toluene (6 mL, 1 M, 6 mmol) was added dropwise. The reaction mixture was stirred overnight, while allowed to reach rt, after which it was quenched with H_2O (200 mL). The organic phase was separated and the aq. phase extracted with CH_2Cl_2 (3 × 150 mL), the combined organics were dried with $MgSO_4$, filtered and concentrated *in vacuo*, which gave a crude 7-bromo-DHA intermediate.

In another flask, a solution of **9** (2.10 g, 7.94 mmol) in THF/MeOH (50 mL, 1 : 1, v/v) was treated with K_2CO_3 (260 mg, 1.88 mmol). The mixture was stirred at rt for 2 h providing **2a** after which the reaction mixture was passed through a plug of silica (40–63 μm, CH_2Cl_2). The mixture was almost concentrated *in vacuo* and redissolved in THF (100 mL) together with the crude 7-bromo-DHA intermediate. The mixture was concentrated to *ca.* 50 mL and flushed with argon. $Pd(PPh_3)_2Cl_2$ (420 mg, 0.60 mmol), CuI (115 mg, 0.60 mmol) and $(iPr)_2NH$ (1.2 mL, 8.6 mmol) were added before the mixture was stirred overnight. The reaction mixture was passed through a plug of silica (40–63 μm, CH_2Cl_2) and then subjected to repeated flash column chromatography (1) (SiO_2 40–63 μm, 60% toluene/heptane to 80% toluene/heptane), (2) (SiO_2 40–63 μm, 20% EtOAc/heptane), (3) (SiO_2 40–63 μm, 20% THF/heptane) which afforded $\mathbf{3a_{NBD–DHA}}$ (243 mg, 0.54 mmol, 9%) as an orange solid. R_f (80% toluene/heptane) = 0.55. R_f (20% EtOAc/heptane) = 0.33. R_f (20% THF/heptane) = 0.20. M.p.: 73–76 °C. ^{1}H NMR (500 MHz, $CDCl_3$) δ 7.81–7.73 (m, 4H), 7.52–7.42 (m, 4H), 7.38 (t, J = 7.7 Hz, 2H), 6.91 (dt, J = 5.0, 2.6 Hz, 1H), 6.89 (s, 1H), 6.86 (dt, J = 5.0, 2.6 Hz, 1H), 6.63 (dt, J = 11.8, 6.1 Hz, 1H), 6.56 (d, J = 11.3 Hz, 1H), 6.34–6.30 (m, 1H), 6.16 (t, J = 4.5 Hz, 1H), 4.05 (m, 1H), 3.87 (td, J = 4.5, 1.7 Hz, 1H), 3.77 (m, 1H), 2.24–2.20 (m, 1H), 2.12 (br d, J = 6.5 Hz, 1H) ppm. ^{13}C NMR (126 MHz, $CDCl_3$) δ 159.4, 159.3, 143.0, 141.3, 141.3, 141.0, 140.5, 140.5, 135.6, 135.6, 132.2, 132.1, 131.8, 131.8, 131.5, 131.4, 130.4, 130.4, 129.5, 129.0, 128.6, 128.0, 126.5, 126.0, 123.8, 123.7, 123.6, 123.6, 120.6, 120.6, 115.1, 115.0, 112.8, 112.7, 99.2, 99.2, 88.3, 88.3, 70.0, 70.0, 57.3, 57.2, 53.4, 53.4, 51.1, 45.1, 45.0 ppm. HR-MS (MALDI + FT-ICR, dithranol): m/z = 447.18656 [M + H$^+$], calcd for [$C_{40}H_{23}N_4^+$]: m/z = 447.18558.

Compound $3b_{NBD–DHA}$ (isolated as a mixture of diastereoisomers). To a solution of **1d** (701 mg, 1.99 mmol) in THF (70 mL) was added acetic acid (1.2 mL, 21 mmol) followed by tetrabutylammonium fluoride (4.0 mL, 1 M in THF, 4.0 mmol). The mixture was stirred for 17 h at rt. The reaction mixture was diluted with Et_2O (200 mL) and quenched with sat. aq. NH_4Cl (100 mL). The organic phase was separated and extracted with sat. aq. NH_4Cl (3 × 100 mL), dried with $MgSO_4$, filtered and concentrated *in vacuo*. The residue was redissolved in THF (60 mL); then **2b** (610 mg, 4.02 mmol) was added, and the mixture was flushed with argon. $Pd(PPh_3)_2Cl_2$ (139 mg, 0.198 mmol), CuI (47 mg, 0.25 mmol) and $(iPr)_2NH$ (0.40 mL, 4.0 mmol) were added before the mixture was stirred overnight. The reaction mixture was passed through a plug of silica (40–63 μm, CH_2Cl_2) and then subjected to flash column

chromatography (SiO_2 40–63 μm, 80% toluene/heptane to 100% toluene), which afforded **6** (32 mg, 0.057 mmol, 6%) as a brown oil and **3b$_{NBD-DHA}$** (82 mg, 0.21 mmol, 10%) as a dark yellow solid. Compound **3b$_{NBD-DHA}$**: R_f (toluene) = 0.33. ^{1}H NMR (500 MHz, $CDCl_3$) δ 7.77–7.73 (m, 2H), 7.51–7.44 (m, 3H), 6.91–6.89 (m, 1H), 6.89–6.81 (m, 2H), 6.70–6.63 (m, 1H), 6.55 (d, J = 11.3 Hz, 1H), 6.36–6.32 (m, 1H), 6.26–6.20 (m, 1H), 3.90–3.87 (m, 1H), 3.87–3.84 (m, 1H), 3.83–3.79 (m, 1H), 2.32–2.27 (m, 1H), 2.21 (ddd, J = 7.1, 3.4, 1.7 Hz, 1H) ppm. ^{13}C NMR (126 MHz, $CDCl_3$) δ 153.7, 153.7, 142.2, 142.2, 141.6, 141.5, 140.3, 132.2, 132.2, 131.7, 131.4, 131.4, 130.6, 130.3, 129.6, 129.5, 129.5, 125.9, 125.9, 122.3, 122.3, 120.7, 116.2, 114.8, 112.7, 105.8, 105.8, 83.1, 83.1, 73.1, 73.0, 57.3, 57.2, 54.3, 54.3, 51.2, 44.9 ppm. HR-MS (MALDI + FT-ICR, dithranol): m/z = 396.14949 [M + H$^+$], calcd for [$C_{28}H_{18}N_3^+$]: m/z = 396.14952. By-product: **6** (isolated as a mixture of diastereoisomers). R_f (toluene) = 0.52. ^{1}H NMR (500 MHz, $CDCl_3$) δ 7.76–7.72 (m, 4H), 7.51–7.44 (m, 6H), 6.89 (s, 2H), 6.64 (dd, J = 11.4, 6.2 Hz, 2H), 6.50 (d, J = 11.4 Hz, 2H), 6.33 (br. d, J = 6.2 Hz, 2H), 6.26 (d, J = 4.8 Hz, 2H), 3.83 (dd, J = 4.8, 1.6 Hz, 2H) ppm. ^{13}C NMR (126 MHz, $CDCl_3$) δ 141.6, 140.2, 132.12, 132.1, 131.6, 131.2, 130.6, 130.2, 129.5, 127.2, 126.5, 121.8, 120.6, 114.8, 112.6, 80.4, 80.4, 73.8, 73.8, 51.1, 44.9 ppm. HR-MS (MALDI + FT-ICR, dithranol): m/z = 559.19266 [M + H$^+$], calcd for [$C_{40}H_{23}N_4^+$]: m/z = 559.19172.

Compound 4a$_{NBD-DHA}$ (isolated as a mixture of diastereoisomers). To a solution of **9** (466 mg, 1.76 mmol) in THF/MeOH (20 mL, 1 : 1, v/v) was added K_2CO_3 (710 mg, 5.14 mmol). The mixture was stirred at rt for 1 h providing **2a** after which the reaction mixture was passed through a plug of silica (40–63 μm, CH_2Cl_2). The mixture was almost concentrated *in vacuo*, then THF (50 mL) was added, and the mixture was again concentrated to 20 mL *in vacuo*. Compound **1b** (455 mg, 1.19 mmol) was added, and the mixture was flushed with argon. $Pd(PPh_3)_2Cl_2$ (82 mg, 0.12 mmol), CuI (24 mg, 0.13 mmol) and (iPr_2)NH (0.25 mL, 1.8 mmol) were added, and the mixture was stirred for 18 h. The mixture was passed through a plug of silica (40–63 μm, CH_2Cl_2) and then subjected to flash column chromatography (50% toluene/heptane to 70% toluene/heptane), which afforded **4a$_{NBD-DHA}$** (331 mg, 0.741 mmol, 62%, based on **1b**) as an orange solid. R_f (70% toluene/heptane) = 0.40. M.p.: Turns sticky at 84 °C, melts fully at 115 °C. ^{1}H NMR (500 MHz, $CDCl_3$): δ 7.88–7.84 (m, 2H), 7.71 (d, J = 8.6 Hz, 2H), 7.54 (d, J = 8.6 Hz, 2H), 7.42 (t, J = 7.5 Hz, 2H), 7.30 (t, J = 7.5 Hz, 1H), 6.96 (dd, J = 5.0, 3.0 Hz, 1H), 6.90 (s, 1H), 6.91–6.89 (m, 1H), 6.57 (dd, J = 11.2, 6.4 Hz, 1H), 6.49 (dd, J = 11.2, 6.1 Hz, 1H), 6.36 (d, J = 6.4 Hz, 1H), 6.32 (ddd, J = 10.2, 6.1, 2.1 Hz, 1H), 5.83 (dd, J = 10.2, 3.8 Hz, 1H), 4.09 (s, 1H), 3.85 (d, J = 2.1 Hz, 1H), 3.80 (dt, J = 3.8, 2.1 Hz, 1H), 2.28 (dt, J = 6.6, 1.5 Hz, 1H), 2.16 (dt, J = 6.6, 1.5 Hz, 1H) ppm. ^{13}C NMR (126 MHz, $CDCl_3$): δ 159.6, 143.1, 141.0, 139.6, 138.7, 135.6, 132.8, 132.0, 131.2, 131.0, 129.8, 129.1, 128.6, 128.1, 127.9, 126.3, 126.2, 125.8, 121.5, 119.6, 115.2, 112.8, 100.5, 91.1, 70.0, 57.4, 53.5, 51.3, 45.2 ppm. HR-MS (ESI + FT-ICR): m/z = 447.18548 [M + H$^+$], calcd for [$C_{33}H_{23}N_2^+$]: m/z = 447.18558.

Compound 4b$_{NBD-DHA}$ (isolated as a mixture of diastereoisomers). To a solution of **1e** (329 mg, 0.933 mmol) in THF (20 mL) was added acetic acid (0.11 mL, 1.9 mmol) followed by tetrabutylammonium fluoride (1.9 mL, 1 M in THF, 1.9 mmol). The mixture was stirred for 2 h at rt, filtered through a plug of silica (40–63 μm, CH_2Cl_2) and almost concentrated *in vacuo*. THF (50 mL) was added, and the mixture was concentrated to approx. 15 mL. Compound **2b** (427 mg, 2.82 mmol) was added, and the mixture was flushed with argon. $Pd(PPh_3)_2Cl_2$ (66 mg, 0.094 mmol), CuI (17 mg, 0.089 mmol) and (iPr)$_2$NH (0.20 mL, 1.4 mmol) were added before the mixture was stirred for 20 h. The mixture was passed through a plug of silica (40–63 μm, CH_2Cl_2) and then subjected to flash column chromatography (SiO_2 40–63 μm, 80% toluene/heptane to 100% toluene), which afforded **7** (69 mg, 0.12 mmol, 13%) as a yellow solid together with impure fractions of **4b$_{NBD-DHA}$**, which were further purified by flash column chromatography (SiO_2 40–63 μm 25% EtOAc/heptane to 30% EtOAc/heptane, loading: toluene), affording **4b$_{NBD-DHA}$** (115 mg, 0.291 mmol, 31%) as a yellow solid. Compound **4b$_{NBD-DHA}$**: R_f (toluene) = 0.37, R_f (30% EtOAc/heptanes) = 0.28. M.p.: 86–91 °C. ^{1}H NMR (500 MHz, $CDCl_3$) δ 7.73 (d, J = 8.6 Hz, 2H), 7.59 (d, J = 8.6 Hz, 2H), 6.95 (s, 1H), 6.91–6.87 (m, 2H), 6.58 (dd, J = 11.2, 6.1 Hz, 1H), 6.50 (dd, J = 11.2, 6.1 Hz, 1H), 6.40–6.37 (m, 1H), 6.32 (ddd, J = 10.2, 6.1, 2.0 Hz, 1H), 5.82 (dd, J = 10.2, 3.8 Hz, 1H), 3.93–3.91 (m, 1H), 3.89–3.87 (m, 1H), 3.80 (dt, J = 3.8, 2.0 Hz, 1H), 2.35 (dt, J = 7.1, 1.5 Hz, 1H), 2.25 (dt, J = 7.1, 1.5 Hz, 1H) ppm. ^{13}C NMR (126 MHz, $CDCl_3$) δ 153.7, 142.3, 141.5, 139.2, 138.5, 133.7, 132.7, 131.5, 131.4, 131.0, 129.6, 127.9, 126.3, 123.6, 122.0, 119.7, 116.3, 115.1, 112.7, 106.8, 85.6, 73.0, 57.3, 54.3, 51.3, 45.1 ppm. HR-MS (ESI + FT-ICR): m/z = 396.14891 [M + H$^+$], calcd for [$C_{28}H_{18}N_3^+$]: m/z = 396.14952. By-product: **7** (isolated as a mixture of diastereoisomers). R_f (toluene) = 0.49. M.p.: >230 °C. ^{1}H NMR (500 MHz, $CDCl_3$): δ = 7.72 (d, J = 8.4 Hz, 2H), 7.63 (d, J = 8.4 Hz, 2H), 6.93 (s, 1H), 6.58 (dd, J = 11.2, 6.2 Hz, 1H), 6.50 (dd, J = 11.2, 6.2 Hz, 1H), 6.39 (m, 1H), 6.35–6.29 (m, 1H), 5.82 (dd, J = 10.2, 3.7 Hz, 1H), 3.83–3.78 (m, 1H) ppm. ^{13}C NMR (126 MHz, $CDCl_3$) δ = 139.2, 138.5, 133.7, 133.4, 131.6, 131.2, 131.0, 127.9, 126.3, 123.3, 122.0, 119.7, 115.1, 112.7, 82.3, 76.5, 51.3, 45.1. HR-MS (ESI + FT-ICR): m/z = 581.17251 [M + H$^+$], calcd for [$C_{40}H_{22}N_4Na^+$]: m/z = 581.17367.

Compound 5a$_{NBD-DHA}$ (isolated as a mixture of diastereoisomers). To a solution of **9** (110 mg, 0.416 mmol) in THF/MeOH (20 mL, 1 : 1, v/v) was added K_2CO_3 (260 mg, 1.88 mmol). The mixture was stirred at rt for 1 h providing **2a** after which the reaction mixture was passed through a plug of silica (40–63 μm, CH_2Cl_2). The mixture was concentrated *in vacuo* and redissolved in THF (20 mL). Compound **1c** (102 mg, 0.267 mmol) was added, and the mixture was flushed with argon. $Pd(PPh_3)_2Cl_2$ (82 mg, 0.12 mmol), CuI (24 mg, 0.13 mmol) and (iPr)$_2$NH (0.05 mL, 0.36 mmol) were added, and the mixture was stirred for 17 h. The mixture was passed through a plug of silica (40–63 μm, CH_2Cl_2) and then subjected to flash column chromatography (60% toluene/heptane to 80% toluene/heptane), which afforded **5a$_{NBD-DHA}$** (61 mg,

0.14 mmol, 51%) as an orange solid. R_f (70% toluene/heptane) = 0.44. M.p.: Gradually decomposes above 101 °C. ^{1}H NMR (500 MHz, $CDCl_3$) δ 7.88–7.84 (m, 2H), 7.80 (m, 1H), 7.70–7.66 (m, 1H), 7.51 (dt, J = 7.7, 1.2 Hz, 1H), 7.45 (t, J = 7.7 Hz, 1H), 7.43–7.39 (m, 2H), 7.29 (t, J = 7.4 Hz, 1H), 6.96 (dd, J = 5.0, 3.0 Hz, 1H), 6.92–6.88 (m, 1H), 6.90 (s, 1H), 6.58 (dd, J = 11.2, 6.2 Hz, 1H), 6.49 (dd, J = 11.2, 6.2 Hz, 1H), 6.36 (d, J = 6.2 Hz, 1H), 6.32 (ddd, J = 10.2, 6.2, 2.0 Hz, 1H), 5.83 (dd, J = 10.2, 3.8 Hz, 1H), 4.09 (m, 1H), 3.86 (m, 1H), 3.80 (dt, J = 3.8, 2.0 Hz, 1H), 2.28 (dt, J = 6.4, 1.5 Hz, 1H), 2.16 (dt, J = 6.4, 1.5 Hz, 1H) ppm. ^{13}C NMR (126 MHz, $CDCl_3$) δ 159.4, 143.1, 141.0, 139.5, 138.6, 135.7, 133.3, 132.6, 131.3, 131.0, 131.0, 129.5, 129.1, 129.0, 128.6, 128.1, 127.8, 126.2, 125.6, 125.4, 121.5, 119.7, 115.1, 112.7, 99.9, 89.4, 70.1, 57.4, 53.5, 51.3, 45.3 ppm. HR-MS (ESI + FT-ICR): m/z = 447.184830 [M + H$^+$], calcd for [$C_{33}H_{23}N_2^+$]: m/z = 447.18558.

Compound $\mathbf{5b_{NBD–DHA}}$ (isolated as a mixture of diastereoisomers). To an argon flushed solution of **2b** (195 mg, 1.29 mmol) and **1f** (555 mg, 1.98 mmol) in THF (24 mL) were added $Pd(PPh_3)_2Cl_2$ (94 mg, 0.13 mmol), CuI (24 mg, 0.13 mmol) and $(iPr)_2NH$ (0.20 mL, 1.4 mmol), and the reaction mixture was stirred for 22 h. The mixture was passed through a plug of silica (40–63 μm, CH_2Cl_2) and then subjected to flash column chromatography (SiO_2 40–63 μm, 50% toluene/heptane to 90% toluene/heptane, loading: toluene), which afforded $\mathbf{5b_{NBD–DHA}}$ (404 mg, 1.02 mmol, 79%) as a dark orange oil and **8** (91 mg, 0.16 mmol, 8% based on **1f**) as a dark orange oil. Compound $\mathbf{5b_{NBD–DHA}}$: R_f (90% toluene/heptane) = 0.26. ^{1}H NMR (500 MHz, $CDCl_3$) δ 7.83–7.81 (m, 1H), 7.77 (d, 7.8 Hz, 1H), 7.56 (d, J = 7.8 Hz, 1H), 7.49 (t, J = 7.8 Hz, 1H), 6.95 (s, 1H), 6.92–6.88 (m, 2H), 6.58 (dd, J = 11.2, 6.2 Hz, 1H), 6.50 (dd, J = 11.2, 6.2 Hz, 1H), 6.38 (d, J = 6.2 Hz, 1H), 6.32 (ddd, J = 10.0, 6.2, 1.9 Hz, 1H), 5.82 (dd, J = 10.0, 3.7 Hz, 1H), 3.94–3.88 (m, 2H), 3.83–3.77 (m, 1H), 2.35 (d, J = 7.0 Hz, 1H), 2.25 (d, J = 7.0 Hz, 1H) ppm. ^{13}C NMR (126 MHz, $CDCl_3$) δ 153.8, 142.2, 141.5, 138.9, 138.4, 133.8, 133.2, 131.4, 131.2, 131.0, 129.7, 129.6, 127.9, 127.0, 123.5, 121.9, 119.6, 116.3, 115.1, 112.6, 106.4, 84.2, 73.1, 57.3, 54.3, 51.3, 45.3 ppm. HR-MS (ESI + FT-ICR): m/z = 396.14900 [M + H$^+$], calcd for [$C_{28}H_{18}N_3^+$]: m/z = 396.14952. By-product: **8** (isolated as a mixture of diastereoisomers). R_f (90% toluene/heptane) = 0.34. ^{1}H NMR (500 MHz, $CDCl_3$) δ 7.89–7.85 (m, 2H), 7.77 (ddd, J = 7.9, 2.0, 1.2 Hz, 2H), 7.61–7.56 (t, J = 7.9, 2H), 7.51–7.45 (m, 2H), 6.93 (s, 2H), 6.58 (dd, J = 11.2, 6.2 Hz, 2H), 6.50 (dd, J = 11.2, 6.2 Hz, 2H), 6.40–6.36 (m, 2H), 6.32 (ddd, J = 10.2, 6.1, 2.1 Hz, 2H), 5.82 (dd, J = 10.2, 3.8 Hz, 2H), 3.80 (dt, J = 3.8, 2.1 Hz, 2H) ppm. ^{13}C NMR (126 MHz, $CDCl_3$) δ 138.9, 138.4, 133.8, 133.7, 131.5, 131.2, 131.0, 130.4, 129.7, 127.9, 126.9, 123.1, 121.9, 119.6, 115.0, 112.6, 81.1, 75.0, 51.3, 45.3 ppm. HR-MS (ESI + FT-ICR): m/z = 557.17846 [M – H$^-$], calcd for [$C_{40}H_{21}N_4^+$]: m/z = 557.17607.

Computations – methods

The photochromic properties of the norbornadiene–dihydroazulene conjugates were theoretically studied by density functional theory (DFT) and its time-dependent analogue (TD-DFT) starting from a comprehensive conformer search. All calculations were performed using Gaussian 16,[22] and structures resulting from geometry optimizations were confirmed as true energy minima through harmonic frequency analyses by the absence of imaginary frequencies. Furthermore, the Gibbs free energy calculations, described in the following, include the zero-point vibrational energy and thermal contributions evaluated at a temperature of 298.15 K and a pressure of 1.00 atm.

The structures shown in Scheme 4 (considering only the *R*-enantiomers of DHA) were initially constructed using GaussView 6,[23] and the geometries were optimized using the hybrid functional B3LYP[24] and the Pople-style 6-311+G(d) basis set.[25] Systematic rotations of 40.0° around the acetylenic part of the two chromophores were then performed, generating 9 distinct conformers of each structure. Subsequently, conformational samplings of the aforementioned conformers were carried out by employing the Confab algorithm implemented using Open Babel 2.4.1[26] with an energy cutoff of 50.0 kcal mol^{-1} and a RMSD cutoff of 0.3 Å. All conformers were then optimized in a vacuum using the semi-empirical PM7 Hamiltonian as modified by Throssel and Frisch. An in-house script ensured that the s-*cis*-VHF and s-*trans*-VHF conformers were correctly categorized, since the two structures mix as a result of the conformer search. The distinct conformers were then identified using a Boltzmann cut-off of 5% and RMSD calculations using the Kabsch algorithm[27] with a tolerance of 0.3 Å.

In order to study the photochromic properties of the molecules, we employed the range-separated hybrid functional CAM-B3LYP[28] and the Pople-style 6-311+G(d) basis set as deemed appropriate in previous benchmark studies[29] and work on similar systems.[5a,20,30] Furthermore, the IEF–PCM continuum solvation model[31] was used to describe polarization effects of toluene through a static and an optical dielectric constant (ε_{st} = 2.374 and ε_{op} = 2.238, respectively). Thus, geometry optimizations and frequency calculations of the distinct conformers allowed us to construct an energy diagram of the different structures, and subsequent TD-DFT calculations of the first 15 excited states enabled us to simulate the UV-Vis spectra (*cf.* ESI†). For the lowest-energy conformers, natural transition orbital (NTO) calculations[32] (an orbital transformation technique) of the strongest transitions were performed, which allowed us to construct more compact illustrations of the orbitals involved in the photoexcitation process.

Conclusions

In conclusion, a series of NBD–DHA conjugates, substituted with phenyl or cyano groups on the NBD, were prepared by Sonogashira couplings of known DHA and NBD starting materials. Linking the two photochromic compounds using a linearly conjugated phenyleneethynylene linker resulted in a red-shifted absorption maximum. All the systems effectively underwent isomerization to the NBD–VHF isomer upon irradiation of the NBD–DHAs. The position of the linker unit

and substituent on the NBD showed to have remarkable effects on the switching properties of the NBD–VHF isomer. Hence, connection through the 7-membered ring resulted in the loss of the photochromism of the NBD moieties in **3a** and **3b**. Interestingly, for the linearly conjugated *para*-linked systems **4a** and **4b**, only the cyano-substituted system **4b** underwent photoisomerization to the QC–VHF isomer. Contrarily, cross-conjugation through the linker (*meta*-phenylene) between NBD and VHF resulted in a possible photoisomerization to the QC–VHF isomers of both the phenyl-substituted **5a** and cyano-substituted **5b**. These findings were rationalized by computational studies by looking at the calculated natural transition orbitals. Moreover, the computational study revealed NBD–VHF conjugates to be (8–10 kJ mol^{-1}) more energetic than NBD–DHA conjugates, while the second isomerization into QC–VHF increased the energy further by 96–101 kJ mol^{-1}. Interestingly, the conjugates exhibit higher energy storage capacities than that corresponding to the sum of the individual photochromic units.

For none of the systems **3–5**, conversion to the QC–DHA isomer could be obtained, as irradiation always resulted in the conversion of DHA into VHF; this, together with the computational study illustrates the need for both NBD and VHF chromophores to be independently optically addressable in order to be able to reach all four different states of the multichromophoric system.

The half-life of the QC moieties was found to be dependent on the solvent, going from 11 min in toluene at 50 °C to only 3 min in CH_2Cl_2 at 25 °C. The fast back-reaction rate of QC in CH_2Cl_2 is in line with our recently observed solvent effects of a related NBD/QC system.[21] It proved impossible to reach the QC–DHA isomer using a previously published Cu(I)-mediated VHF-to-DHA conversion method. However, the addition of Cu (I) changed the VHF-to-DHA back-reaction to occur on the same time scale as that of the QC-to-NBD conversion. The absence or presence of Cu(I) is thus a convenient way of tuning heat release rates on different or identical time scales of QC–VHF conjugates.

The synthesis presented here, using the Sonogashira reaction in the key coupling step, allows for great modularity in the molecular design and enables the design of future multichromophoric systems with optimised solar capture efficiencies and application-optimized thermal energy release rates.

Conflicts of interest

Q6 ■■■■

Acknowledgements

We thank the University of Copenhagen for financial support. N. R. thanks H.C. Ørsted Selskabet and Ørsted A/S for financial support in terms of the Ørsted Scholarship 2018.

Notes and references

1 (*a*) T. J. Kucharski, Y. Tian, S. Akbulatov and R. Boulatov, *Energy Environ. Sci.*, 2011, **4**, 4449; (*b*) K. Moth-Poulsen, D. Ćoso, K. Börjesson, N. Vinokurov, S. K. Meier, A. Majumdar, K. P. C. Vollhardt and R. A. Segalman, *Energy Environ. Sci.*, 2012, **5**, 8534; (*c*) A. Lennartson, A. Roffey and K. Moth-Poulsen, *Tetrahedron Lett.*, 2015, **56**, 1457; (*d*) L. Dong, Y. Feng, L. Wang and W. Feng, *Chem. Soc. Rev.*, 2018, **47**, 7339.

2 (*a*) Z. Yoshida, *J. Photochem.*, 1985, **29**, 27; (*b*) K. Börjesson, A. Lennartson and K. Moth-Poulsen, *ACS Sustainable Chem. Eng.*, 2013, **1**, 585.

3 (*a*) A. M. Kolpak and J. C. Grossman, *Nano Lett.*, 2011, **11**, 3156; (*b*) E. Durgun and J. C. Grossman, *J. Phys. Chem. Lett.*, 2013, **4**, 854; (*c*) T. J. Kucharski, N. Ferralis, A. M. Kolpak, J. O. Zheng, D. G. Nocera and J. C. Grossman, *Nat. Chem.*, 2014, **6**, 441; (*d*) E. N. Cho, D. Zhitomirsky, G. G. D. Han, Y. Liu and J. C. Grossman, *ACS Appl. Mater. Interfaces*, 2017, **9**, 8679; (*e*) G. G. D. Han, H. Li and J. C. Grossman, *Nat. Commun.*, 2017, **8**, 1446; (*f*) J. Huang, Y. Jiang, J. Wang, C. Li and W. Luo, *Thermochim. Acta*, 2017, **657**, 163.

4 (*a*) A. Dreos, K. Börjesson, Z. Wang, A. Roffey, Z. Norwood, D. Kushnir and K. Moth-Poulsen, *Energy Environ. Sci.*, 2017, **10**, 728; (*b*) M. Mansø, A. U. Petersen, Z. Wang, P. Erhart, M. B. Nielsen and K. Moth-Poulsen, *Nat. Commun.*, 2018, **9**, 1945; (*c*) Z. Wang, A. Roffey, R. Losantos, A. Lennartson, M. Jevric, A. U. Petersen, M. Quant, A. Dreos, X. Wen, D. Sampedro, K. Börjesson and K. Moth-Poulsen, *Energy Environ. Sci.*, 2019, **12**, 187.

5 (*a*) M. H. Hansen, J. Elm, S. T. Olsen, A. N. Gejl, F. E. Storm, B. N. Frandsen, A. B. Skov, M. B. Nielsen, H. G. Kjaergaard and K. V. Mikkelsen, *J. Phys. Chem. A*, 2016, **120**, 9782; (*b*) Z. Wang, J. Udmark, K. Börjesson, R. Rodrigues, A. Roffey, M. Abrahamsson, M. B. Nielsen and K. Moth-Poulsen, *ChemSusChem*, 2017, **10**, 3049; (*c*) M. D. Kilde, P. G. Arroyo, A. S. Gertsen, K. V. Mikkelsen and M. B. Nielsen, *RSC Adv.*, 2018, **8**, 6356.

6 (*a*) R. Boese, J. K. Cammack, A. J. Matzger, P. Pflug, W. B. Tolman, K. P. C. Vollhardt and T. W. Weidman, *J. Am. Chem. Soc.*, 1997, **119**, 6757; (*b*) Y. Kanai, V. Srinivasan, S. K. Meier, K. P. C. Vollhardt and J. C. Grossman, *Angew. Chem., Int. Ed.*, 2010, **49**, 8926; (*c*) J. Gurke, M. Quick, N. P. Ernsting and S. Hecht, *Chem. Commun.*, 2017, **53**, 2150; (*d*) K. Edel, X. Yang, J. S. A. Ishibashi, A. N. Lamm, C. Maichle-Mössmer, Z. X. Giustra, S.-Y. Liu and H. F. Bettinger, *Angew. Chem., Int. Ed.*, 2018, **57**, 5296; (*e*) G. Ganguly, M. Sultana and A. Paul, *J. Phys. Chem. Lett.*, 2018, **9**, 328. Q7

7 (*a*) A. U. Petersen, S. L. Broman, S. T. Olsen, A. S. Hansen, L. Du, A. Kadziola, T. Hansen, H. G. Kjaergaard, K. V. Mikkelsen and M. B. Nielsen, *Chem. – Eur. J.*, 2015, **21**, 3968; (*b*) A. Vlasceanu, S. L. Broman, A. S. Hansen, A. B. Skov, M. Cacciarini, A. Kadziola, H. G. Kjaergaard, K. V. Mikkelsen and M. B. Nielsen, *Chem. – Eur. J.*, 2016,

22, 10796; (*c*) A. Vlasceanu, B. N. Frandsen, A. B. Skov, A. S. Hansen, M. G. Rasmussen, H. G. Kjaergaard, K. V. Mikkelsen and M. B. Nielsen, *J. Org. Chem.*, 2017, **82**, 10398.

8 (*a*) J. Daub, T. Knöchel and A. Mannschreck, *Angew. Chem., Int. Ed. Engl.*, 1984, **23**, 960; (*b*) S. L. Broman, S. L. Brand, C. R. Parker, M. Å. Petersen, C. G. Tortzen, A. Kadziola, K. Kilså and M. B. Nielsen, *ARKIVOC*, 2011, **ix**, 51.

9 (*a*) L. Gobbi, P. Seiler and F. Diederich, *Angew. Chem., Int. Ed.*, 1999, **38**, 674; (*b*) L. Gobbi, P. Seiler, F. Diederich, V. Gramlich, C. Boudon, J.-P. Gisselbrecht and M. Gross, *Helv. Chim. Acta*, 2001, **84**, 743.

10 S. L. Broman, M. Jevric, A. D. Bond and M. B. Nielsen, *J. Org. Chem.*, 2014, **79**, 41.

11 S. L. Broman, M. Å. Petersen, C. G. Tortzen, A. Kadziola, K. Kilså and M. B. Nielsen, *J. Am. Chem. Soc.*, 2010, **132**, 9165.

12 M. Santella, V. Mazzanti, M. Jevric, C. R. Parker, S. L. Broman, A. D. Bond and M. B. Nielsen, *J. Org. Chem.*, 2012, **77**, 8922.

13 A. U. Petersen, M. Jevric and K. Moth-Poulsen, *Eur. J. Org. Chem.*, 2018, 4465.

14 M. Quant, A. Lennartson, A. Dreos, M. Kuisma, P. Erhart, K. Börjesson and K. Moth-Poulsen, *Chem. – Eur. J.*, 2016, **22**, 13265.

15 M. Å. Petersen, S. L. Broman, A. Kadziola, K. Kilså and M. B. Nielsen, *Eur. J. Org. Chem.*, 2009, 2733.

16 C. R. Parker, C. G. Tortzen, S. L. Broman, M. Schau-Magnussen, K. Kilså and M. B. Nielsen, *Chem. Commun.*, 2011, **47**, 6102.

17 M. Cacciarini, A. Vlasceanu, M. Jevric and M. B. Nielsen, *Chem. Commun.*, 2017, **53**, 5874.

18 Z. Wang, A. Roffey, R. Losantos, A. Lennartson, M. Jevric, A. U. Petersen, M. Quant, A. Dreos, X. Wen, D. Sampedro, K. Börjesson and K. Moth-Poulsen, *Energy Environ. Sci.*, 2019, **12**, 187.

19 (*a*) C. Slavov, C. Yang, L. Schweighauser, C. Boumrifak, A. Dreuw, H. A. Wegner and J. Wachtveitl, *Phys. Chem. Chem. Phys.*, 2016, **18**, 14795; (*b*) C. Yang, C. Slavov, H. A. Wegner, J. Wachtveitl and A. Dreuw, *Chem. Sci.*, 2018, **9**, 8665.

20 N. Ree, M. H. Hansen, A. S. Gertsen and K. V. Mikkelsen, *J. Phys. Chem. A*, 2017, **121**, 8856.

21 M. Quant, A. Hamrin, A. Lennartson, P. Erhart and K. Moth-Poulsen, *J. Phys. Chem. C*, 2019, **123**, 7081.

22 M. J. Frisch, *et al.*, *Gaussian 16 Revision A.03*, Gaussian Inc., Wallingford CT, 2016.

23 R. Dennington, T. A. Keith and J. M. Millam, *GaussView, Version 6*, Semichem Inc., Shawnee Mission, KS, 2016.

24 A. D. Becke, *J. Chem. Phys.*, 1993, **98**, 5648.

25 (*a*) W. J. Hehre, R. Ditchfield and J. A. Pople, *J. Chem. Phys.*, 1972, **56**, 2257; (*b*) J. S. Binkley, J. A. Pople and W. J. Hehre, *J. Am. Chem. Soc.*, 1980, **102**, 939; (*c*) R. Krishnan, J. S. Binkley, R. Seeger and J. A. Pople, *J. Chem. Phys.*, 1980, **72**, 650.

26 N. M. O'Boyle, M. Banck, C. A. James, C. Morley, T. Vandermeersch and G. R. Hutchison, Open Babel: An open chemical toolbox, *J. Cheminf.*, 2011, **3**, 33.

27 (*a*) W. Kabsch, *Acta Crystallogr., Sect. A: Cryst. Phys., Diffr., Theor. Gen. Crystallogr.*, 1976, **32**, 922; (*b*) Calculate root-mean-square deviation (RMSD) of Two Molecules Using Rotation, GitHub, http://github.com/charnley/rmsd, <0c8e9ec552b3596b0a69f90ef54b8304e1309df1>.

28 T. Yanai, D. P. Tew and N. C. Handy, *Chem. Phys. Lett.*, 2004, **393**, 51.

29 (*a*) S. T. Olsen, J. Elm, F. E. Storm, A. N. Gejl, A. S. Hansen, M. H. Hansen, J. R. Nikolajsen, M. B. Nielsen, H. G. Kjaergaard and K. V. Mikkelsen, *J. Phys. Chem. A*, 2015, **119**, 896; (*b*) M. J. Kuisma, A. M. Lundin, K. Moth-Poulsen, P. Hyldgaard and P. Erhart, *J. Phys. Chem. C*, 2016, **120**, 3635.

30 N. Ree, C. L. Andersen, M. D. Kilde, O. Hammerich, M. B. Nielsen and K. V. Mikkelsen, *Phys. Chem. Chem. Phys.*, 2018, **20**, 7438.

31 (*a*) S. Miertuš, E. Scrocco and J. Tomasi, *Chem. Phys.*, 1981, **55**, 117; (*b*) E. Cances, B. Mennucci and J. Tomasi, *J. Chem. Phys.*, 1997, **107**, 3032.

32 R. L. Martin, *J. Chem. Phys.*, 2003, **118**, 4775.